TESTS OF COLD-FORMED STAINLESS STEEL CHS-TO-SHS HYBRID TUBULAR JOINTS

RAN FENG[1] and YUEXIN LIU[1]

[1]*School of Civil and Environmental Engineering, Harbin Institute of Technology, Shenzhen, China.*
E-mail: fengran@hit.edu.cn

A test program was conducted on cold-formed stainless steel CHS-to-SHS hybrid tubular T-, Y- and X-joints made of circular braces and square chord. The failure modes, failure strengths and deformation curves were obtained from experimental investigation. The influences of geometrical parameters including the brace diameter/chord width ratio (β), the brace/chord thickness ratio (τ), the chord width/thickness ratio (2γ) and the inclined angle (θ) between brace and chord on the failure strengths of all specimens were carefully evaluated. Experimental results show that the initial stiffnesses and the failure strengths of all specimens increased with the increment of the β value, and increased with the decrement of the θ value. However, the influences of τ and 2γ are insignificant. Furthermore, the test strengths are compared with the nominal design strengths calculated using the design formulae of the current design guidelines including CIDECT, Eurocode 3 (EC3), Australian/New Zealand Standard (AS/NZS) and Chinese Code, in which AS/NZS is the only design guideline for stainless steel structures. The comparison indicates that the design formulae of EC3 are most conservative. While, the design formulae of AS/NZS are generally appropriate for cold-formed stainless steel CHS-to-SHS hybrid tubular joints.

Keywords: CHS-to-SHS hybrid joint, Circular brace, Square chord, Stainless steel.

1 Introduction

Tubular structures are one of the widely used structural forms employed in the on-shore and off-shore structures, in which circular, square and rectangular hollow sections (CHS, SHS and RHS) are the most commonly used tubes in tubular structures. The tubular joints at the intersection of tubular members are the most critical components govern the failure of tubular structures. There are various forms of tubular joints in connection of various shapes of tubular members, in which the CHS tubular joint was formed at the intersection of CHS tubes, the SHS or RHS tubular joint was formed at the intersection of SHS or RHS tubes, and the hybrid tubular joint was formed at the intersection of CHS and SHS or RHS tubes. It is worth noting that the CHS-to-SHS or RHS hybrid tubular joint fabricated from CHS brace members and SHS or RHS chord member exhibits some unique advantages, such as no complex intersecting line cutting, and better fatigue life due to less stress concentrations occurred. Nowadays, stainless steel is being used increasingly for structural purposes because of its advantages over carbon steel, such as attractive appearance, better corrosion resistance, excellent durability, ease of maintenance and low cost in service life. However, the increasing use of stainless steel tubes in tubular structures and the lack of researches on stainless steel tubular joints are in sharp contrast.

Proceedings of the 17th International Symposium on Tubular Structures.
Editors: X.D. Qian and Y.S. Choo

Published by Research Publishing, Singapore.
ISBN: 978-981-11-0745-0; doi:10.3850/978-981-11-0745-0_079-cd

The behavior of carbon steel tubular joints were extensively investigated, and the researches were ever performed on tubular T-, Y- and X-joints in carbon steel at various loading conditions of static loading (Zhao 2000), combined static loading actions (Zhao and Hancock 1991) and fatigue loading (Chiew et al. 2007), as well as chord preload at elevated temperatures (Shao et al. 2016). Whereas, the researches on stainless steel tubular joints are relatively few. A series of researches were conducted by Feng and Young (2008, 2010, 2011, 2012, 2013, 2015) on stainless steel SHS and RHS tubular T- and X-joints under static loading. The experimental, numerical and theoretical analyses were performed to evaluate the effects of critical parametric variables. Reasonable design guidelines were provided for the failure criteria, joint strengths and stress concentrations of stainless steel tubular joints. However, few studies were reported on hybrid tubular joints, let alone stainless steel hybrid tubular joints. Based on the authors' knowledge, no research was ever conducted on stainless steel hybrid tubular joints.

An experimental investigation was conducted in this study on cold-formed stainless steel CHS-to-SHS hybrid tubular T-, Y- and X-joints fabricated from circular braces and square chord. The influences of the key geometrical parameters including the brace diameter/chord width ratio (β), the brace/chord thickness ratio (τ), the chord width/thickness ratio (2γ) and the inclined angle (θ) between brace and chord on the axial compressive capacities of stainless steel hybrid tubular joints were evaluated. The test strengths are compared with the nominal design strengths obtained from four current design guidelines to verify the applicability of each guideline to the design of stainless steel CHS-to-SHS hybrid tubular T-, Y- and X-joints.

2 Experimental work

There are 18 stainless steel hybrid tubular joints in the test program, which include 4 T-, 5 Y- and 9 X-joints (5 X-joints with θ of 90° and 4 X-joints with θ of 45°) with the schematic diagrams displayed in Fig. 1. All specimens were precisely fabricated with the axes of braces passing through the center of chord axis. The measured specimen sizes and geometrical parameters including the brace diameter/chord width ratio ($\beta=d_1/b_0$), the brace/chord thickness ratio ($\tau=t_1/t_0$), the chord width/thickness ratio ($2\gamma=b_0/t_0$), and the inclined angle (θ) between brace and chord are summarized in Table 1. The labeling system of the specimens in Table 1 is established based on the joint form and cross-section sizes. For instance, the first letter 'T', 'Y' and 'X' indicates T-, Y- and X-joint, respectively. The second part of the labeling system represents the cross-section sizes of square chord and the third part of the labeling system represents the cross-section sizes of circular brace. All specimens were made from austenitic stainless steel AISI 304. The mechanical properties of the stainless steel SHS and CHS tubes are summarized in Table 2, which include the Young's modulus (E), the yield stress ($\sigma_{0.2}$) and the ultimate stress (σ_u) of the material, and the elongation after fracture (ε_f).

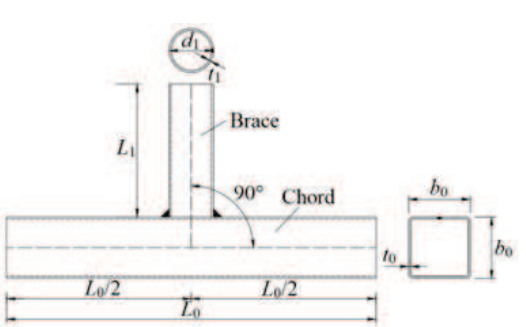

(a) T-joint

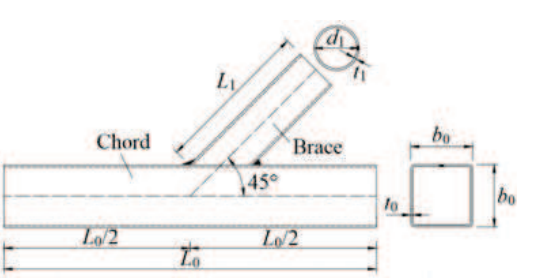

(b) Y-joint

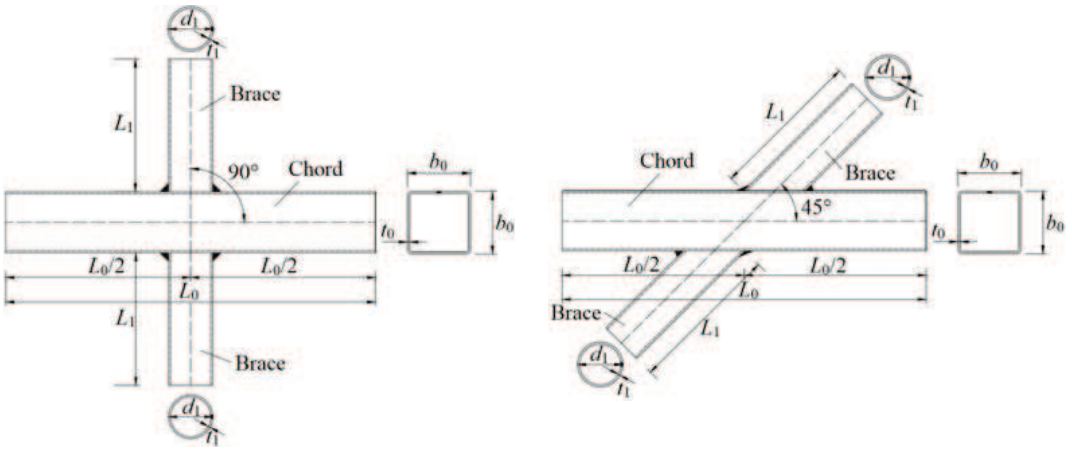

(c) X-joint (θ=90°) (d) X-joint (θ=45°)

Figure 1. Schematic diagrams of different forms of tubular joints

Table 1. Measured specimen sizes and geometrical parameters of stainless steel hybrid tubular joints

Specimen	Chord (mm)			Brace (mm)			Geometrical parameter		
	b_0	t_0	L_0	d_1	t_1	L_1	β	τ	2γ
T-C150×3-B108×3	150.23	3.014	900	108.43	3.044	325	0.72	1.01	49.84
T-C150×3-B133×3	149.99	3.022	900	132.08	3.036	400	0.88	1.00	49.63
T-C200×4-B108×3	200.15	3.957	1200	108.83	3.094	325	0.54	0.78	50.58
T-C200×4-B133×3	199.79	3.815	1200	131.23	2.884	400	0.66	0.76	52.37
Y-C150×3-B108×3	150.57	2.906	900	108.29	2.845	325	0.72	0.98	51.81
Y-C150×3-B108×3-R	150.05	2.991	900	108.32	2.792	325	0.72	0.93	50.17
Y-C150×3-B133×3	149.80	3.000	900	131.72	3.046	400	0.88	1.02	49.93
Y-C200×4-B108×3	199.56	3.949	1200	108.39	3.044	325	0.54	0.77	50.53
Y-C200×4-B133×3	199.44	3.993	1200	132.16	3.031	400	0.66	0.76	49.95
X-C150×3-B108×3	149.93	2.960	900	108.39	3.048	325	0.72	1.03	50.65
X-C150×3-B133×3	149.81	2.966	900	131.76	3.001	400	0.88	1.01	50.51
X-C150×3-B133×3-R	149.80	2.958	900	131.83	2.999	400	0.88	1.01	50.64
X-C200×4-B108×3	199.90	3.971	1200	108.42	3.065	325	0.54	0.77	50.34
X-C200×4-B133×3	199.44	3.975	1200	131.44	3.016	400	0.66	0.76	50.17
X-C150×3-B108×3-45°	150.05	3.007	900	107.86	2.828	325	0.72	0.94	49.90
X-C150×3-B133×3-45°	149.71	2.956	900	132.12	2.995	400	0.88	1.01	50.65
X-C200×4-B108×3-45°	200.06	3.970	1200	108.50	3.058	325	0.54	0.77	50.39
X-C200×4-B133×3-45°	199.58	4.038	1200	131.61	3.032	400	0.66	0.75	49.43

Table 2. Mechanical properties of stainless steel tubes

Section	E (MPa)	$\sigma_{0.2}$ (MPa)	σ_u (MPa)	ε_f (%)	$\sigma_{0.2}/\sigma_u$
□150×3	207009	430.27	780.20	57.34	0.55
□200×4	188370	423.71	758.11	54.34	0.56
○108×3	232622	441.15	750.12	54.52	0.59
○133×3	229172	433.96	753.36	63.17	0.58

The test setup of stainless steel CHS-to-SHS hybrid tubular joints is given in Fig. 2. The hydraulic jack was vertically placed on the top end plate of circular brace to apply axial compression with a load cell placed in between. Both ends of the square chord of stainless steel hybrid tubular T- and Y-joints were pin-connected to the bottom supports by the high strength steel hinges, which were fixed on the ground floor by anchor bolts. Hence, the boundary conditions that both ends of the square chord could rotate along the in-plane direction in the compression tests were effectively implemented. Unlike hybrid tubular T- and Y-joints, both ends of the square chord of hybrid tubular X-joints are free. The bottom end plate of lower brace member was bolted on a fixed-ended spherical bearing, which was specially designed to ensure that the loading application on hybrid tubular X-joints was pure axial compression without bending moment. The compression tests were conducted by using the multi-stage loading procedure for all specimens, which were loaded monotonically first by load control prior to the reach of the ultimate strengths and followed by displacement control in the post-ultimate stage.

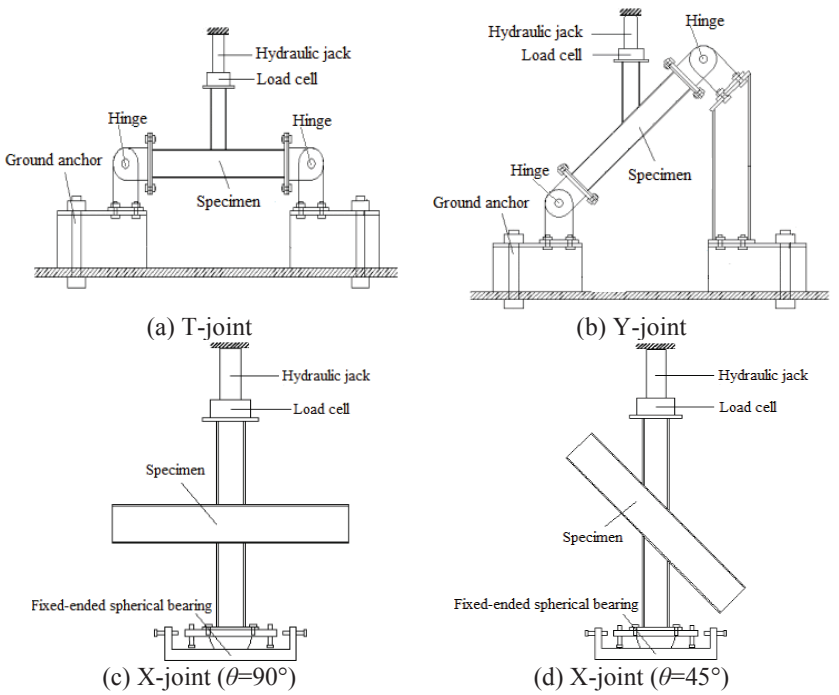

Figure 2. Test setup of stainless steel hybrid tubular joints

3 Test results and discussions

Two typical failure modes including chord face plastification and chord side wall failure were observed from the compression tests of stainless steel CHS-to-SHS hybrid tubular T-, Y- and X-joints, as shown in Fig. 3, which are also listed in Table 3 for all specimens, except for the specimen X-C150×3-B133×3-45° that subjected to premature failure. The chord face plastification usually occurred for stainless steel hybrid tubular joints with the β value ranged from 0.6 to 0.8. The plastic zone of chord flange was fully developed with the occurrence of the stress redistribution, which resulted in the failure of the chord face. The chord side wall failure usually occurred for stainless steel hybrid tubular joints with the β value close to 1. The loads applied to the braces were transmitted directly to the chord webs, which eventually resulted in the chord side wall failure.

Table 3. Test results and comparison results for stainless steel hybrid tubular joints

Specimen	β	Failure mode	N_{Test} (kN)	N_{Test} /N_{nCI}	N_{Test} /N_{nEC}	N_{Test} /$N_{nA/N}$	N_{Test} /N_{nCC}
T-C150×3-B108×3	0.72	A	42.28	1.08	1.20	0.98	1.20
T-C150×3-B133×3	0.88	B	74.71	1.20	1.34	0.83	1.03
T-C200×4-B108×3	0.54	A	53.82	1.25	1.39	1.13	1.39
T-C200×4-B133×3	0.66	A	66.65	1.28	1.42	1.15	1.43
Y-C150×3-B108×3	0.72	A	61.24	1.02	1.14	0.92	1.14
Y-C150×3-B108×3-R	0.72	A	60.02	0.95	1.05	0.85	1.05
Y-C150×3-B133×3	0.88	B	119.31	1.16	1.29	0.77	1.01
Y-C200×4-B108×3	0.54	A	68.51	1.01	1.13	0.91	1.12
Y-C200×4-B133×3	0.66	A	113.98	1.23	1.37	1.11	1.36
X-C150×3-B108×3	0.72	A	38.92	1.03	1.15	0.93	1.15
X-C150×3-B133×3	0.88	B	85.17	1.47	1.63	0.98	1.31
X-C150×3-B133×3-R	0.88	B	80.34	1.39	1.55	0.93	1.24
X-C200×4-B108×3	0.54	A	48.03	1.11	1.23	1.00	1.23
X-C200×4-B133×3	0.66	A	53.06	0.94	1.04	0.85	1.04
X-C150×3-B108×3-45°	0.72	A	68.92	1.08	1.19	0.97	1.20
X-C200×4-B108×3-45°	0.54	A	72.65	1.06	1.18	0.96	1.18
X-C200×4-B133×3-45°	0.66	A	102.32	1.08	1.21	0.97	1.20

Note: A=Chord face plastification; B=Chord side wall failure.

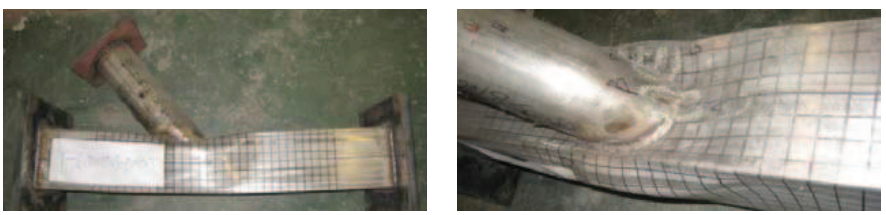

(a) Chord face plastification

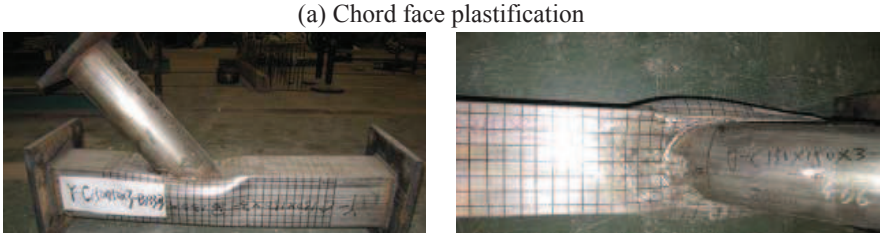

(b) Chord side wall failure

Figure 3. Typical failure modes of stainless steel tubular Y-joints

The axial load versus chord deformation curves of stainless steel CHS-to-SHS hybrid tubular T-joints are illustrated in Fig. 4. It is found that the deformation curves of stainless steel hybrid tubular joints with the β value of 0.88 exhibit the clear peak load, whereas there is no clear peak load in the deformation curves of stainless steel hybrid tubular joints with the β value less than 0.88, which may attribute to the post-yield response caused by the membrane force in the chord flange and strain hardening property of stainless steel material. Furthermore, the initial stiffnesses of stainless steel hybrid tubular joints increased with the increment of the β value, but insignificantly influenced by other geometrical parameters of τ and 2γ.

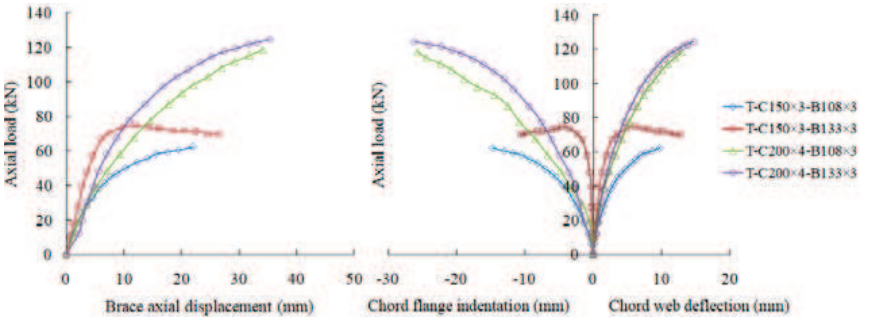

Figure 4. Axial load versus chord deformation curves of stainless steel tubular T-joints

The failure strengths (N_{Test}) of stainless steel hybrid tubular joints are listed in Table 3. The influences of the key geometrical parameters on the failure strengths of stainless steel hybrid tubular joints were investigated in Fig. 5. It is found that the failure strengths of stainless steel hybrid tubular joints increased with the increment of the β value. The comparison also shows that the failure strengths of stainless steel hybrid tubular Y-joints are larger than those of stainless steel hybrid tubular T-joints with the same geometrical sizes. In addition, the failure strengths of stainless steel hybrid tubular X-joints with θ of 45° are larger than those of stainless steel hybrid tubular X-joints with θ of 90° with the same geometrical sizes. Therefore, the failure strengths of stainless steel hybrid tubular joints increased with the decrement of the θ value.

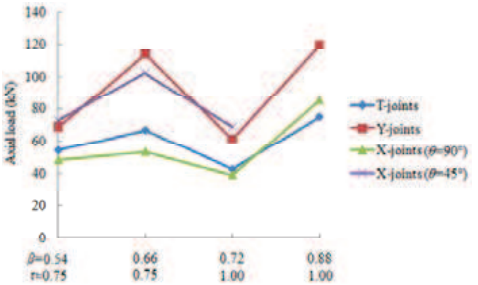

Figure 5. Comparison of failure strengths with different key geometrical parameters

4 Design guidelines

This paper introduces four different design guidelines namely CIDECT (2009), Eurocode 3 (EC3 2005), Australian/New Zealand Standard (AS/NZS 2001) and Chinese Code (2017) to determine the load-carrying capacities of stainless steel hybrid tubular joints fabricated from circular braces and square chord. Among these design guidelines, CIDECT (2009), EC3 (2005) and Chinese Code (2017) were designed for carbon steel structures, while AS/NZS (2001) was designed for stainless steel structures. It should be noted that the inclined angle (θ) between brace and chord was defined to be greater than 30º in these design guidelines.

The nominal design strengths (N_{nCI}) of hybrid tubular joints with circular braces and square chord can be obtained from Eqs. (1) and (2) given in CIDECT (2009) as follows:

For $\beta \leq 0.85$,
$$N_{nCI} = \left(\frac{2\beta}{(1-\beta)\sin\theta} + \frac{4}{\sqrt{1-\beta}} \right) \frac{\pi f_{y0} t_0^2}{4\sin\theta} Q_f / 0.9 \quad (1)$$

For $\beta = 1.0$,
$$N_{nCI} = \left(\frac{2d_1}{\sin\theta} + 10t_0 \right) Q_f \frac{\pi f_k t_0}{4\sin\theta} / 0.9 \quad (2)$$

where Q_f=1 is the influential factor for chord stresses on the load-carrying capacities, f_k is the flexural buckling stress of chord web which is equal to χf_{y0} and $0.8\chi f_{y0}\sin\theta$ for tubular T/Y-joints and X-joints with brace in compression, respectively, where χ is the reduction factor for column buckling based on the relevant buckling curve and slenderness, and f_{y0} is the yield stress of chord.

The nominal design strengths (N_{nEC}) of hybrid tubular joints with circular braces and square chord can be obtained from Eqs. (3) and (4) given in EC3 (2005) as follows:

For $\beta \leq 0.85$,
$$N_{nEC} = \frac{\pi k_n f_{y0} t_0^2}{4(1-\beta)\sin\theta}\left(\frac{2\beta}{\sin\theta} + 4\sqrt{1-\beta}\right) \tag{3}$$

For β=1.0,
$$N_{nEC} = \frac{\pi f_k t_0}{4\sin\theta}\left(\frac{2d_1}{\sin\theta} + 10t_0\right) \tag{4}$$

where k_n=1 is the influential factor for chord stresses on the load-carrying capacities, f_k is the flexural buckling stress of chord web, f_{y0} is the yield stress of chord.

It should be noted that the linear interpolation between the load-carrying capacities at β=0.85 and at β=1.0 needs to be used for $0.85<\beta<1.0$. Furthermore, the load-carrying capacities in CIDECT (2009) and EC3 (2005) need to be limited by a reduction factor of 0.9 under the condition of f_{y0}>355 N/mm.

The nominal design strengths ($N_{nA/N}$) of hybrid tubular joints with circular braces and square chord can be obtained from Eq. (5) given in AS/NZS (2001) as follows:

For $\beta \leq 0.85$,
$$N_{nA/N} = \frac{\pi f_{y0} t_0^2}{4(1-\beta)\sin\theta}\left(\frac{2\beta}{\sin\theta} + 4(1-\beta)^{0.5}\right)\left(\frac{k_n}{0.9}\right) \tag{5}$$

In this paper, the load-carrying capacities of the specimens with β=0.88 were also obtained from the design equation for hybrid tubular joints with $\beta \leq 0.85$.

The nominal design strengths (N_{nCC}) of hybrid tubular joints with circular braces and square chord can be obtained from Eqs. (6) and (7) given in Chinese Code (2017) as follows:

For $\beta \leq 0.85$,
$$N_{nCC} = 1.8\left(\frac{\beta}{(1-\beta)^{0.5}\sin\theta} + 2\right)\frac{\pi f_{y0} t_0^2}{4(1-\beta)^{0.5}\sin\theta}\psi_n \tag{6}$$

For β=1.0,
$$N_{nCC} = 2.0\left(\frac{d_1}{\sin\theta} + 5t_0\right)\frac{\pi t_0 f_k}{4\sin\theta}\psi_n \tag{7}$$

where ψ_n=1 is the influential factor for chord stresses on the load-carrying capacities. The linear interpolation between the load-carrying capacities at β=0.85 and at β=1.0 needs to be used for $0.85<\beta<1.0$.

The comparison of test strengths (N_{Test}) with nominal design strengths (N_{nCI}, N_{nEC}, $N_{nA/N}$ and N_{nCC}) is summarized in Table 3. The mean values of test/nominal design strength ratios (N_{Test}/N_{nCI}, N_{Test}/N_{nEC}, $N_{Test}/N_{nA/N}$ and N_{Test}/N_{nCC}) are 1.14, 1.27, 0.96 and 1.19, with the coefficients of variation (COVs) of 0.148, 0.165, 0.104 and 0.126 for CIDECT (2009), EC3 (2005), AS/NZS (2001) and Chinese Code (2017), respectively. The comparison indicates that the design formulae of CIDECT (2009), EC3 (2005) and Chinese Code (2017) are all conservative, in which the design formulae of EC3 (2005) are most conservative with the largest value of COV. While, the design formulae of AS/NZS (2001) are generally appropriate for cold-formed stainless steel CHS-to-SHS hybrid tubular joints with the smallest value of COV.

5 Conclusions

(1) The initial stiffnesses and the failure strengths of stainless steel hybrid tubular joints increased with the increment of the β value, and increased with the decrement of the θ value. However, the influences of other geometrical parameters of τ and 2γ on the initial stiffnesses and the failure strengths are insignificant.
(2) Most of the specimens failed by chord face plastification and no clear peak load was observed from the deformation curves. Whereas, some other specimens with the large β value failed by chord side wall and the clear peak load was obtained from the deformation curves.
(3) The design formulae of CIDECT and Chinese Code are conservative, and the design formulae of EC3 are most conservative. While, the design formulae of AS/NZS are generally appropriate for cold-formed stainless steel CHS-to-SHS hybrid tubular joints.

Acknowledgments

The authors are grateful for the financial support from National Natural Science Foundation of China (Grant No. 51528803), Natural Science Foundation of Guangdong Province of China (Grant No. 2018A030313208), State Key Laboratory of Subtropical Building Science (South China University of Technology, Grant No. 2018ZA02), and Guangdong Provincial Key Laboratory of Durability for Marine Civil Engineering, Shenzhen Durability Center for Civil Engineering (Shenzhen University, Grant No. GDDCE 18-5). The tests were conducted in Anhui Key Lab on Structure and Material of Civil Engineering at Hefei University of Technology. The support provided by the laboratory staff is gratefully acknowledged.

References

Australian/New Zealand Standard (AS/NZS), *Cold-Formed Stainless Steel Structures*, AS/NZS 4673: 2001, Sydney, Australia, 2001.

Chiew, S. P., Lee, C. K., Lie, S. T., Ji, H. L., Fatigue Behaviors of Square-to-Square Hollow Section T-Joint with Corner Crack. I: Experimental Studies, *Eng. Fract. Mech.*, 74(5), 703-720, March, 2007.

Chinese Code, *Code for Design of Steel Structures*, GB 50017-2017, Beijing, China, 2017. (in Chinese)

CIDECT Guide No. 3. *Design Guide for Rectangular Hollow Section (RHS) Joints under Predominantly Static Loading*. 2nd ed., Comité International pour le Développement et l'Étude de la Construction Tubulaire (CIDECT), Geneva, Switzerland, 2009.

Eurocode 3 (EC3), *Design of Steel Structures − Part 1-8: Design of Joints*, European Committee for Standardization, EN 1993-1-8: 2005, CEN. Brussels, Belgium, 2005.

Feng, R. and Young, B., Experimental Investigation of Cold-Formed Stainless Steel Tubular T-Joints, *Thin. Wall. Struct*., 46(10), 1129-1142, October, 2008.

Feng, R. and Young, B., Tests and Behaviour of Cold-Formed Stainless Steel Tubular X-Joints, *Thin. Wall. Struct*., 48(12), 921-934, December, 2010.

Feng, R. and Young, B., Design of Cold-Formed Stainless Steel Tubular T- and X-Joints, *J. Constr. Steel. Res*., 67(3), 421-436, March, 2011.

Feng, R. and Young, B., Design of Cold-Formed Stainless Steel Tubular Joints at Elevated Temperatures, *Eng. Struct*., 35, 188-202, February, 2012.

Feng, R. and Young, B., Stress Concentration Factors of Cold-Formed Stainless Steel Tubular X-joints, *J. Constr. Steel. Res*., 91(12), 26-41, December, 2013.

Feng, R. and Young, B., Theoretical Analysis of Cold-Formed Stainless Steel Tubular Joints. *Eng. Struct*., 83, 99-115, January, 2015.

Shao, Y. B., Zheng, Y. J., Zhao, H. C., Yang, D. P., Performance of Tubular T-Joints at Elevated Temperature by Considering Effect of Chord Compressive Stress, *Thin. Wall. Struct*., 98, 533-546, January, 2016.

Zhao, X. L. and Hancock, G. J., T-Joints in Rectangular Hollow Sections Subject to Combined Actions, *J. Sruct. Eng-ASCE*., 117(8), 2258-2277, August, 1991.

Zhao, X. L., Deformation Limit and Ultimate Strength of Welded T-Joints in Cold-Formed RHS Sections, *J. Constr. Steel. Res*., 53(2), 149-165, February, 2000.